A Microfluidic Device with an Integrated Waveguide Beam Splitter for Velocity Measurements of Flowing Particles by Fourier Transformation

ARTICLE *in* ANALYTICAL CHEMISTRY · OCTOBER 2003

Impact Factor: 5.64 · DOI: 10.1021/ac034427a · Source: PubMed

6 AUTHORS, INCLUDING:

Klaus B Mogensen
Philips
54 PUBLICATIONS **1,563** CITATIONS
SEE PROFILE

Jan C T Eijkel
University of Twente
158 PUBLICATIONS **3,719** CITATIONS
SEE PROFILE

Nickolaj Jacob Petersen
University of Copenhagen
24 PUBLICATIONS **512** CITATIONS
SEE PROFILE

Jörg P Kutter
University of Copenhagen
161 PUBLICATIONS **3,533** CITATIONS
SEE PROFILE

Anal. Chem. **2001,** *73,* 1748−1753

Velocity Measurement of Particles Flowing in a Microfluidic Chip Using Shah Convolution Fourier Transform Detection

Yien C. Kwok, Nicholas T. Jeffery, and Andreas Manz*

AstraZeneca/SmithKline Beecham Centre for Analytical Sciences, Department of Chemistry, Imperial College of Science, Technology and Medicine, London SW7 2AY, United Kingdom

A noninvasive radiative technique, based on Shah convolution Fourier transform detection, for velocity measurement of particles in fluid flows in a microfluidic chip, is presented. It boasts a simpler instrumental setup and optical alignment than existing measurement methods and a wide dynamic range of velocities measurable. A glass−PDMS microchip with a layer of patterned Cr to provide multiple detection windows which are 40 μm wide and 70 μm apart is employed. The velocities of fluorescent microspheres, which were electrokinetically driven in the channel of the microfluidic chip, were determined. The effects of increasing the number of detection windows and sampling period were investigated. This technique could have wide applications, ranging from the determination of the velocity of particles in pressure-driven flow to the measurement of electrophoretic mobilities of single biological cells.

The study of solid particles in liquid or gas flows is of increasing importance in biology and in industrial processes. In biology, numerous solid−liquid systems exist, for example, blood. Industrial examples include fuel injection in combustion engines, aerosols and solid particulate flow in smoke stacks, and fluidized beds; understanding the flow characteristics would aid in the design and control of such processes.

For the measurement of particulate velocities, the technique being employed has to be noninvasive, be able to probe the bulk medium, and possess the capability of constant monitoring. Satisfying most of these constraints, radiative methods remove the need for disruption of the system by physical sampling or insertion of a probe in the flow. Hence, it is no wonder to find most, if not all, techniques are radiative in principle. Three different measurement principles are generally used, namely, correlation, the Doppler effect, and spatial filtering.

In temporal correlation techniques, the velocity is inversely proportional to the transit time taken for flow tracers to cross a fixed distance. This includes the two-slit photometric method[1] and the dual-window videodensitometric technique.[2] In spatial correlation techniques, the velocity is directly proportional to the displacement of flow tracers in a fixed time interval. Video techniques[3] based on this principle have been developed over the years for measuring first centerline velocities inside tubes and later velocity profiles.[4] However, the maximum velocity measurable is limited by the frame rate of the video. Laser Doppler techniques rely on the Doppler shift of laser light as a wave strikes a moving object.[5] It is the same principle used in "radar" guns, enabling police to measure the speed of passing traffic. However, if the velocity of the moving object is small, the Doppler shift will be too small for the even highest resolution spectrometers to cope. The third class of velocity measurement techniques is based on the principle of spatial filtering. Two laser beams of equal intensity are focused and crossed at the point of interest where a laser interference pattern is created. As a particle moves through, a periodic signal will be obtained at a detector, the frequency of this being proportional to the velocity of the scatterer.[5] Combining the laser Doppler anemometer with a microscope to form a laser Doppler microscope anemometer could increase spatial resolution.[6]

Velocity measurement, as applied to particles that are electrokinetically mobilized, allows the qualitative assessment of the adsorption of polymeric surfactants onto polystyrene particles[7] and size-based characterization of colloidal gold nanoparticles.[8] In biology, the measurement of the velocity of cells moving under the influence of an electric field is important. The intrinsic electrophoretic mobilities (EPMs) of cells could reveal whether the cells under different physiological conditions or exposed to different physiologically active agents would have an altered net surface charge as reflected by their different EPMs. Three primary methodologies are available—microelectrophoresis, laser Doppler technology, and free flow electrophoresis.[9] In free flow electrophoresis, the electric field is applied perpendicular to the flow stream, whereas, the applied field is parallel to the flow for electrophoresis. Of these three methodologies, the direct measurement of cell EPM by free flow electrophoresis is difficult, as

* Corresponding author: (e-mail) a.manz@ic.ac.uk; (fax) +44-207-594 5833.

(1) Wayland, H.; Johnson, P. C. *J. Appl. Phys.* **1967**, *22*, 333−337.
(2) Intaglietta, M.; Silverman, N. R.; Tompkins, W. R. *Microvasc. Res.* **1975**, *10*, 165−179.
(3) Goodman, A. H.; Guyton, A. C.; Drake, R.; Loflin, J. H. *J. Appl. Physiol.* **1974**, *37*, 126−130.
(4) Alonso, C.; Pries, A. R.; Kiesslich, O.; Lerche, D.; Gaehtgens, P. *Am. J. Physiol.* **1995**, *268*, H25−32.
(5) Drain, L. E. *The Laser Doppler Technique*; Wiley: Chichester, U.K., 1980.
(6) Einav, S.; Berman, H. J.; Fuhro, R. I.; DiGiovanni, P. R.; Fine, S.; Fridman, J. D. *Biorheology* **1975**, *12*, 203−205.
(7) Huff, B. V.; McIntire, G. L. *J. Microcolumn Sep.* **1994**, *6*, 591−594.
(8) Schnabel, U.; Fischer, C. H.; Kenndler, E. *J. Microcolumn Sep.* **1997**, *9*, 529−534.
(9) Slivinsky, G. G.; Hymer, W. C.; Bauer, J.; Morrison, D. R. *Electrophoresis* **1997**, *18*, 1109−1119.

10.1021/ac0013047 CCC: $20.00
Published on Web 03/07/2001

it could only be estimated on the basis of elution positions with red blood cells as the reference standards.[10] Differences in the surface properties of Gram positive and negative cells have been studied by the measurement of their EPMs.[11] EPMs have also been used for the diagnosis of diabetes[12] and gynecological malignancies.[13]

A survey of the existing methods for the velocity measurement of particles or cells in fluid flows reveals a number of problems. The accuracy and reproducibility of the results obtained by correlation methods are highly dependent on the spacing of the two detection points and the length of the integration period of the cross-correlation. Laser Doppler methods require complicated and expensive instrumentation, involving difficult and precise optical alignment of the laser beam, optical lenses, and photodetector. Free flow electrophoresis, being a relative method, requires calibration with red blood cells. Last, invasive methods, which place a probe in the flow, can cause disruption and affect the accuracy of the velocity measurements.

A detection system comprising a new method of column interrogation and a corresponding domain for analytical separation data presentation based on a convolution of the detection function similar to the Shah function, followed by Fourier transform (FT), was proposed by Crabtree et al., who named this technique Shah convolution Fourier transform detection, or SCOFT.[14] Further work was performed by Kwok and Manz.[15] During the separation, each analyte band progressing along the column at its characteristic speed produces a series of evenly spaced Gaussian peaks, and the time-domain signal is thus the resultant sum of these several series of Gaussian peaks, *n* series for *n* analytes. FT in the forward direction yields the frequency components that are contained in the time-domain signal. This technique has been successfully demonstrated for a separation. Similar to the work by Crabtree et al.,[14] this work is performed on a microfluidic chip[16] because it offers the obvious advantage in the ease with which the channel and detection slits can be fabricated and aligned to each other. The microfluidic device offers real or expected benefits in terms of analytical figures of merit such as separation time and plate number and in terms of portability and automation as well as reagent and instrumentation cost.[17] Microspheres are used in microfluidic devices for DNA hybridization[18] and immunoassay.[19]

In this paper, a noninvasive radiative technique for the velocity measurement of solid particles in fluid flows in a microfluidic chip is described. The principle of the measurement technique is based on SCOFT.[14,15] The effects of the number of detection windows and sampling period were also studied.

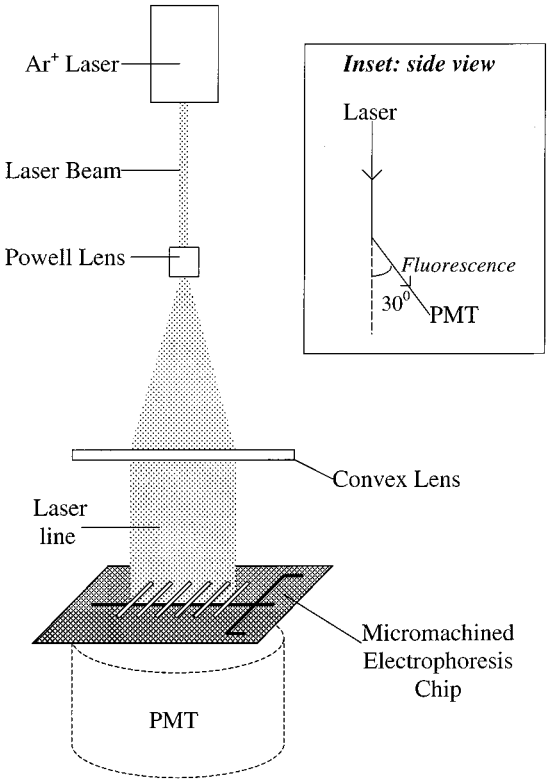

Figure 1. Instrumental setup (inset is the side view of the setup).

EXPERIMENTAL SECTION

Apparatus. Figure 1 shows a schematic of the instrumentation. The lenses, laser, chip, and electrodes were mounted with lens mounts or custom-made fixtures on carriers along a vertically mounted 2-m optical rail (lens mounts and posts on an X-95 rail and carrier system, Newport, Irvine, CA); the photomultiplier tube (PMT) was mounted in a ring stand. The whole apparatus was enclosed in a light-tight galvanized steel box. A 13-mW argon ion laser (line at 488 nm; model 532-B-A01, OmNichrome (Melles Griot), Chino, CA) was shone initially upon a single Powell-10-0.75 lens (Elliot Scientific, Herts, U.K.) followed by a convex cylindrical lens (01LCP009, $f = 80$ mm, Melles Griot) placed ~4.5 cm below. The chip was aligned and positioned ~7.5 cm beneath the convex lens. This laser line was ~2 cm long and ~100 μm wide on the chip. The chip was held in the apparatus with a locally built holder which fixes the chip in the optical path and the Pt electrodes in the reservoirs and provides high-voltage contacts for the electrodes.

Detection was performed with a 5.1-cm-diameter head-on PMT (R550 PMT, E1198-11 socket, C3830 power supply, Hamamatsu Photonics, Middlesex, U.K.) with three high-pass interference filters (505EFLP, Omega Optical, Brattleboro, VT), three high-pass Schott filters (OG515, Edmund Scientific, Barrington, NJ), and one fluorescein emission band-pass filter (520DF15, Omega Optical) attached to the PMT, the last next to the PMT. The filter edges and PMT−filter interface were carefully foil-wrapped to eliminate unfiltered light from reaching the PMT. The PMT−filter assembly was positioned beneath the chip at an angle of ~30° from the plane of the laser beam and was spaced ~3.5 cm from the center of the detection area.

Current signal from the PMT biased at −1000 V was first filtered with a low-pass filter (VBF21M, Kemo, Kent, U.K.) set at

(10) Hannig, K. *Electrophoresis* **1982**, *3*, 235−243.
(11) Sonohara, R.; Muramatsu, N.; Ohshima, H.; Kondo, T. *Biophys. Chem.* **1995**, *55*, 273−277.
(12) Kitagawa, S.; Nozaki, O.; Tsuda, T. *Electrophoresis* **1999**, *20*, 2560−2565.
(13) Hoffmann, W.; Werner, W.; Steiner, R.; Kaufmann, R. *Br. J. Cancer* **1981**, *43*, 588−597.
(14) Crabtree, H. J.; Kopp, M. U.; Manz, A. *Anal. Chem.* **1999**, *71*, 2130−2138.
(15) Kwok, Y. C.; Manz, A. *Electrophoresis* **2001**, *22*, 222−229.
(16) Manz, A.; Graber, N.; Widmer, H. M. *Sens. Actuators, B* **1990**, *1*, 244−248.
(17) Kopp, M. U.; Crabtree, H. J.; Manz, A. *Curr. Opin. Chem. Biol.* **1997**, *1*, 410−419.
(18) Fan, Z. H.; Mangru, S.; Granzow, R.; Heaney, P.; Ho, W.; Dong, Q.; Kumar R. *Anal. Chem.* **1999**, *71*, 4851−4859.
(19) Sato, K.; Tokeshi, M.; Odake, T.; Kimura, H.; Ooi, T.; Nakao, M.; Kitamori, T. *Anal. Chem.* **2000**, *72*, 1144−1147.

40-Hz cutoff frequency. The output from the low-pass filter was then measured using a PICO analog digital convertor (ADC, Pico Instruments) data acquisition system with the scan rate set at 100 Hz. Data manipulation and fast Fourier transforms (FFTs) were performed using Igor Pro 3 (Wavemetrics, Lake Oswego, OR) with Microsoft Excel 5.0 after acquisition.

Potentials at the four electrodes were controlled by a home-made power supply, wherein discrete dc−dc converters (one per electrode) were regulated via multiplexing from a LabView program (National Instruments, Austin, TX) running on an Apple Power Macintosh 9500/120. This allowed effective switching of all four electrodes in ~300 ms and electrical current sourcing or sinking at any electrode, as well as independent current and voltage monitoring.

Microfluidic Chip. In view of possible blockages, a glass−poly(dimethylsiloxane) (PDMS) chip was decided. This combination of materials allows the chip to be disassembled for cleaning, followed by assembly for later use.

The microfluidic chip was fabricated in-house using standard photolithography and etching techniques[20] on 7.6 cm × 7.6 cm soda lime glass substrates (Nanofilm, Westlake, CA). The channels were ~10.5 μm deep, 36 μm wide at the top, and 15 μm wide at the bottom. The top plate was made of PDMS. Hole reservoirs of ~2 mm in diameter were bored in a 7.6 cm × 7.6 cm × ~0.2 cm thick piece of PDMS top plate. This was subsequently aligned and laid onto the glass substrate with the etched channel system. The slit array was fabricated on a third piece of 0.25-cm-thick glass substrate coated with a layer of ~1000-Å-thick Cr; the Cr layer was patterned to provide 375 detection windows which were each 40 μm wide and spaced 70 μm center to center (or the sum of the widths of a detection window and an adjacent gap is 70 μm). The center of the slit array was roughly aligned with the midpoint between the intersection and buffer waste reservoir. Figure 2 is a schematic diagram of the chip and slit array layout used in this work—a simple cross pattern of two intersecting channels and four reservoirs: (a) the sample injection channel with sample and sample waste reservoirs and (b) the separation channel with buffer and buffer waste reservoirs, above which the detection slit array lays. Channel lengths, measured from the intersection, were 5 mm to the sample reservoir, 37 mm to the buffer reservoir, 43 mm to the sample waste, and 57 mm to the buffer waste.

Reagents and Solutions. Tris−Borate−EDTA (TBE) buffer was prepared at 0.1× concentration (8.9 mM each of tris-(methoxy)aminomethane and boric acid, 0.2 mM in ethylenediaminetetraacetic acid; prepared from a solid TBE mixture, Fluka) with deionized water (water purification system, Elga Ltd., Bucks, U.K.) and filtered through 0.2-mm filters (Millisart). With the use of TBE buffer, aggregation of microspheres and adhesion of microspheres to the channel wall were almost completely removed. Appropriate amounts of sodium fluorescein (salt, Fluka) was dissolved in 0.1× TBE to make a 150 μM fluorescein in 0.1× TBE solution. Fluorescent polystyrene microspheres, amine-modified, 1.0-μm diameter, yellow-green (505/515), 2% solids were supplied by Molecular Probes Europe B. V. Cleaning solution of 0.5 M sodium hydroxide was prepared from deionized water and sodium hydroxide (BDH).

(20) Sirichai, S.; de Mello, A. J. *Analyst* **2000**, *125*, 133−137.

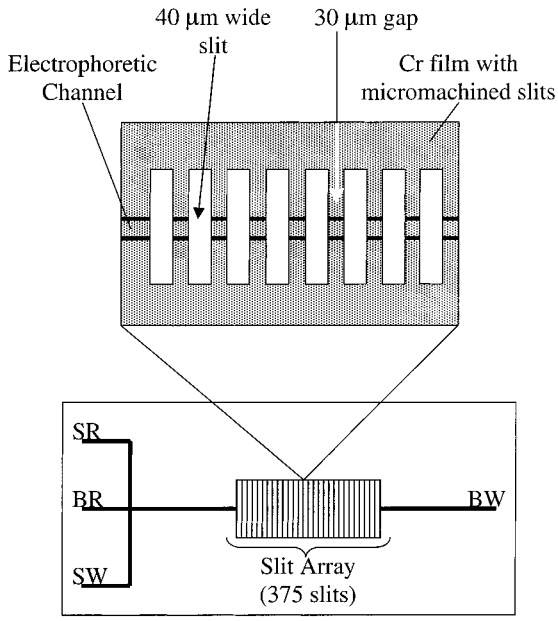

Figure 2. Schematic diagram of the micromachined electrophoresis chip showing the electrophoretic channels and the patterned Cr layer which provides the multiple detection windows. (SR, sample reservoir; BR, buffer reservoir; SW, sample waste; BW, buffer waste).

Preparatory and Experimental Procedure. A 0.002% (~3.6×10^6 microspheres/mL) fluorescent microspheres sample solution was prepared by diluting the stock sample (2%) by 1000-fold with 0.1× TBE buffer. All fluorescent microspheres sample solutions were sonicated prior to use to reduce aggregation. To prepare the chip, cleaning fluids were drawn into the chip by applying vacuum to one reservoir and supplying the other three with the appropriate fluid. Daily chip preparation consisted of drawing through 0.5 M NaOH followed by the running buffer, 0.1× TBE. The sample solution was then loaded into the sample reservoir, the three other reservoirs were filled with 0.1× TBE buffer, and the chip was ready to run. For overnight storage, the chip was filled with deionized water.

Fluorescein solution was placed into the sample reservoir and drawn into the separation channel by suction at the buffer waste reservoir, while buffer solution was supplied to the remaining three reservoirs. Then the sample reservoir was emptied of fluorescein solution and replaced by the 0.002% fluorescent microspheres sample solution, and the buffer waste reservoir was filled with the buffer solution. The electrophoretic channel, now filled with the fluorescein solution which was previously drawn into the channel, was aligned with the laser line. The high-voltage protocol, as shown in Table 1, was run. The first step purged the fluorescein solution (for aligning) out of the channel into the buffer waste reservoir, and the second step would continuously mobilize the fluorescent microspheres from the sample reservoir into the channel to be detected. Mixing of the buffer and sample solution occurred in the second step but would only moderately dilute the microspheres sample solution. This does not affect the velocity measurement of the microspheres. The concentration of fluorescent microspheres in the sample solution used was very low, ~3.6×10^6 microspheres/mL, such that each microsphere moved independently across the detection area with the estimated

Table 1. Typical High-Voltage Program Used for Measuring the Velocities of the Microspheres

	reservoir potential (V)				
step	sample	buffer	sample waste	buffer waste	time (s)
fluorescein purge	1500	3000	1500	0	180
microspheres mobilization	1800	1800	1500	1100	600

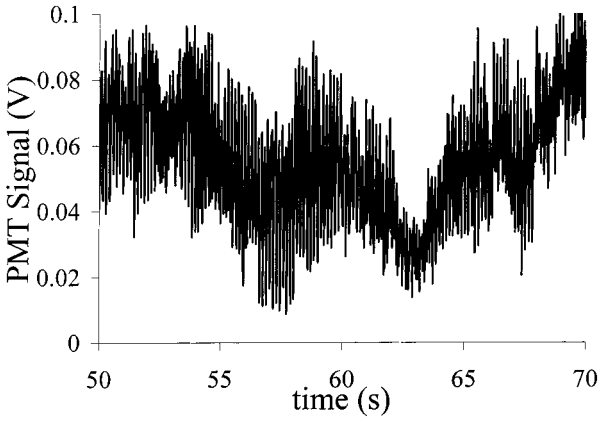

Figure 3. Time-domain detector signals collected when the fluorescent microspheres were introduced into the detection area (50 slits). Part (20 s) of the 120-s sampling period was shown for clarity. Conditions: 0.1× TBE buffer, pH 8.4; electric field strength 161 V/cm.

distance between each microsphere being 1 mm. The time-domain signal was then recorded.

Only part of the slit array (of 375 detection windows) was used at any one time. The slit array was covered with aluminum foil, only exposing the exact number of detection windows to be used for each experiment.

Data Analysis. Data points were acquired and stored as text files in PICO and processed using Igor Pro 3. Time, $t = 0$ for the time-domain signals, was arbitrarily selected within the 600-s period of the second step of Table 1, and data for an even number of points bracketing the relevant time span were then treated with a FFT in the forward direction to yield the frequency-domain data. No apodization function was employed. The FFT algorithm yields $(N/2) + 1$ complex points (pairs of real, $FT_{v,\,Re}$, and imaginary points, $FT_{v,\,Im}$) in the frequency domain for an input of N real points in the time domain. These complex data can also be represented in terms of their magnitude, $FT_{v,\,Mag}$:

$$FT_{v,Mag} = \sqrt{(FT_{v,Re})^2 + (FT_{v,Im})^2} \qquad (1)$$

The magnitude of noise in the frequency domain was estimated as the peak-to-peak averaged over a range of 2 Hz (around the fundamental peak) and was subsequently used to calculate the signal-to-noise ratio (S/N) in the frequency domain.

RESULTS AND DISCUSSION

Figure 3 displays an example of the time-domain signal when 50 40-μm-wide slits were used. Subsequent FT yielded the magnitude (eq 1) plot in the frequency domain, as shown in Figure 4. A fundamental peak with a S/N of 16 can be seen. The center frequency of the fundamental peak, in Figure 4A, was 7.1 Hz. This translates to a velocity of (7.1 Hz × 70 μm) 497 μm/s. In the case

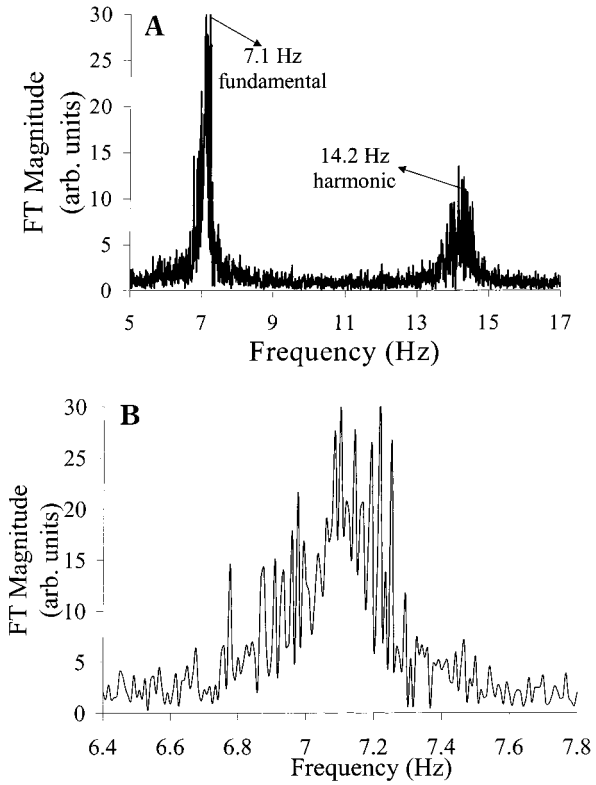

Figure 4. (A) Fourier transformation of Figure 3, displayed in magnitude formats. (B) An expanded view of the 7.1-Hz fundamental peak in (A).

where the frequency of the fundamental peak is f and the center-to-center spacing between detection windows is d, the velocity of the particles, u, can be defined by eq 2. This clearly demonstrates

$$u = fd \qquad (2)$$

the applicability of SCOFT as a new method for the measurement of velocity of particles or the like, for example, biological cells. The dynamic range of measurable velocities can be extended by increasing the spacing between the detection windows, and theory suggests that the range could also be extended by increasing the rate of data acquisition (to satisfy the Nyquist criteria of FT).[21] The part of Figure 4A containing the fundamental peak was expanded for clarity, and this is shown in Figure 4B. A series of narrow peaks with the center/maximum around 7.1 Hz could be seen. Each narrow peak represents a particular velocity. This is because, within the sampling period, more than one microsphere moved under the detection area and there exists a distribution of charge-to-size ratio of the microspheres used. Hence, a distribution of velocities was determined, with the center/mean frequency at

(21) Marshall, A. G.; Verdun, F. R. *Fourier Transforms in NMR, Optical, and Mass Spectrometry. A User's Handbook*; Elsevier: Amsterdam, 1990.

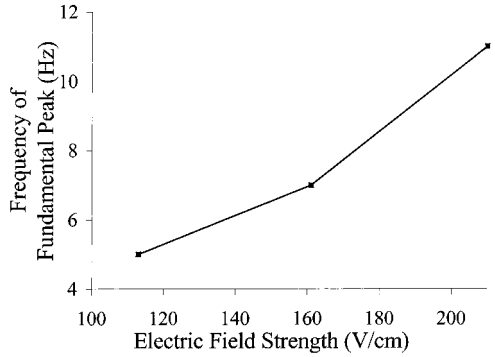

Figure 5. Frequency of the fundamental peak at various electric field strengths.

7.1 Hz. By sampling a statistically significant number of particles, the velocity distribution of the microspheres could be determined. A rough estimate, based on the concentration of microspheres in the sample solution used for the experiment, showed that there were ~70 microspheres moving within the detection area over a sampling period of 120 s. Hence, the time-domain signal, shown in Figure 3, was a summation of fluorescence from ~70 microspheres, i.e., 70 × 50 measurements. However, in Figure 4B, there were only ~20 narrower peaks centering around 7.1 Hz. It is probable that some microspheres have the same velocity, or similar velocity, such that the small difference is indistinguishable by this method. It is believed and highly probable that SCOFT is still applicable even if there exists, for example, a bimodal distribution of sizes and/or charges. In addition, in Figure 4A, the magnitude of the first harmonics (at ~14.2 Hz) relative to the fundamental peak (at 7.1 Hz) was observed to be much greater than that obtained by Crabtree et al.[14] Crabtree et al. reported the observation of stronger harmonics than experimentally observed results when a computer simulation of a series of Gaussian peaks was performed. However, the effect of band-broadening of the sample plug on the FT results was not considered by Crabtree et al. Since band-broadening is absent for individual microsphere, band-broadening may be responsible for the observed difference in the relative magnitude of the first harmonics to the fundamental peak. Efforts to find ways to reduce or eliminate the strong first harmonics should be undertaken, as the first harmonics is a potential interference if another fundamental peak were to occur at or near to the position of a first harmonics of the other fundamental peak. According to FT theory,[22] the first harmonics could be removed if the width of the detection windows is half of the center-to-center separation distance between adjacent detection windows, for example, 35-μm-wide detection windows with a center-to-center spacing of 70 μm.

Figure 5 shows the effect of the electric field strength on the frequency of the fundamental peak. It can be seen that the frequency of the fundamental peak increases with the electric field strength. An increase in electric field strength increases the electroomostic flow velocity of the bulk solution and the electrophoretic velocity of the microspheres. The end result is an increase in the net velocity of the microspheres, which is clearly reflected by the corresponding increase in the frequency of the fundamental peak. This demonstrates the response of SCOFT to the change in the net velocity of the microspheres flowing in the microchannel by the frequency shift of the fundamental peak. The same approach could be taken to measure the velocity of particles in pressure-driven flows.

The effect of the number of detection windows was studied. Using 50, 100, and 150 detection windows which were 40 μm wide, time-domain signals were collected over 120 s. After FT, results similar to those in Figure 4 were obtained. The S/Ns were calculated and found to be 15.8, 15.4, and 16 when 50, 100, and 150 detection windows were used, respectively. There was no significant difference in the S/N of the fundamental peak when a different number of detection windows was used. The effect of the sampling period was also investigated. With fifty 40-μm-wide detection windows, the time-domain signals was collected over 120, 240, and 480 s. After FT, the results also resembled Figure 4. The S/N's were 15.8, 15.2, and 15 for the sampling periods of 120, 240, and 480 s, respectively. Similarly, there was no significant difference in the S/N of the fundamental peak. Therefore, increasing the number of detection windows and/or sampling period do not seem to offer any further advantage in terms of S/N.

CONCLUSIONS

A noninvasive radiative technique for the velocity measurement of particles in fluid flows in a microfluidic chip has been successfully demonstrated. The principle employed was Shah convolution Fourier transform detection, which is a form of spatial filtering. This technique involves simpler instrumentation than laser Doppler methods (which require difficult and precise optical alignment). The frequency of the fundamental peak is sensitive to changes in the net velocity of the microspheres. Future work will focus on the removal/reduction of the relatively strong first harmonics which could interfere with the measurements.

Decreasing the size of the detection windows to study its effect on the FT results and the accuracy and reproducibility of the velocity measurements will also be considered. A particle could be likened to a molecule and be used to model the response of a molecule by SCOFT. Therefore, it would shed light on the potential of the SCOFT technique to detect and measure the velocities of a single molecule flowing in the channel of a microfluidic device.

Though having been demonstrated for microspheres moving in a microfluidic device, the described SCOFT principle would be equally applicable to measure the velocities of sand, dust, or any solid particles in fluid flows in any channel system. EPMs of biological cells could be determined by the same SCOFT principle, with the possibility of establishing the EPM distribution if a significant number of cells were to be sampled. It is proposed that the height of the fundamental peak in the frequency domain could be related to the number of cells and, hence, could provide a qualitative, if not quantitative, method of cell counting.

Research on SCOFT has just begun in the last couple years. Results and applications have been reported, but SCOFT is expected to have more to offer. It is believed that SCOFT may promise more exciting capabilities and applications which could benefit the scientific world.

(22) James, J. F. *A Student's Guide to Fourier Transforms: with Applications in Physics and Engineering* Athenaeum Press: Newcastle upon Tyne, U.K., 1995.

ACKNOWLEDGMENT

The clean-room facility used for fabrication of the microchip was financially supported by BBSRC, AstraZeneca, and SmithKline Beecham. The authors thank Dr. H. J. Crabtree for his help and guidance in the project. The authors also thank Drs. J.C.T. Eijkel, G.H.W. Sanders, R. Tantra, and C.X. Zhang for all the insightful discussions, Dr. Elisabeth K. Hill for her help with the laser optics, and finally Mr. Gareth Jenkins for assistance in microchip fabrication. Y.C.K. acknowledges the funding from the Overseas Research Student Awards Scheme and the financial support from his parents.

Received for review November 6, 2000. Accepted January 28, 2001.

AC0013047